

Synthesis of pH-Responsive Core-Shell Nanoparticles of Different Sizes and with Different Shell Compositions

by

Jason S Pellegrino

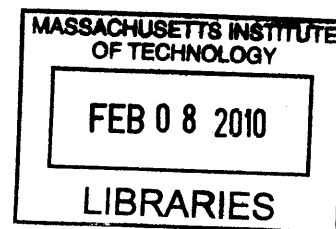
Submitted to the Department of Material Science and Engineering
On May 16, 2008 in Partial Fulfillment of the
Requirements for the Degree of

Bachelor of Science

at the

Massachusetts Institute of Technology

June 2008



ARCHIVES

© 2008 Jason Pellegrino
All rights reserved

The author hereby grants to MIT permission to reproduce and to
distribute publicly paper and electronic copies of this thesis document in whole or in part
in any medium now known or hereafter created.

Handwritten signature of Jason S. Pellegrino in black ink.

Signature of Author.....
Department of Materials Science and Engineering
May 16, 1989

Certified by
7V - - - - 4
Darrell J. Irvine
Associate Professor of Material Science & Engineering and Biological Engineering
Thesis Supervisor

Accepted by
Caroline A. Ross
Chair, Undergraduate Committee

Synthesis of pH-Responsive Core-Shell Nanoparticles of Different Sizes and with Different Shell Compositions

by

Jason S Pellegrino

Submitted to the Department of Material Science and Engineering
On May 16, 2008 in Partial Fulfillment of the
Requirements for the Degree of
Bachelor of Science

ABSTRACT

The endosome-disrupting and pH-responsive poly(2-diethylamino ethyl methacrylate)-core/poly(2-aminoethyl methacrylate)-shell nanoparticles could potentially increase the efficacy of transcutaneous administered vaccines and facilitate the cytosolic delivery of a wide variety of therapeutic macromolecules.

One of the goals of this study was to reduce the size of these core-shell nanoparticles to improve their permeation into the skin. Separate nanoparticle syntheses using reduced durations, decreased monomer concentrations, and decreased monomer solubility did not cause a significant decrease in the particle diameter compared to those previously reported. Manipulation of the reaction kinetics did not stabilize smaller particles leaving them susceptible to coagulation. Synthesis of poly(2-diethylamino ethyl methacrylate)/ Poly(ethylene glycol) methacrylate copolymer nanoparticles were sterically stabilized by the amphiphilic polymer brush at the particle surface and exhibited slightly smaller hydrodynamic diameter measured by dynamic light scattering. Manipulation of the reaction kinetics and the monomer ratio could lead to significantly smaller chains.

Another goal for this study was to create core-shell nanoparticles with different charged shells to see if the shell could be modified to electrostatically adsorb a wider range of drugs. In addition, the different charges of the shell could affect the nanoparticles' endosome-disrupting abilities and/or their permeation through the skin. Surprisingly, the zeta-potential measurements were the same for each sample though the shells were supposed to have different charges. This suggests that surface charge density of the PDEAEMA core was being measured. When nanoparticles with a smaller PDEAEMA core and a thicker PAEMA shell were synthesized, a change in the zeta potential was observed that was consistent with the larger positive surface charge density and the higher pK_b of the PAEMA shell. This suggests that the adsorption of positively charged drugs may be difficult because it would require negatively charged shell that is thick enough to counteract the positive PDEAEMA core.

Thesis Supervisor: Darrell J. Irvine

Title: Associate Professor of Material Science & Engineering and Biological Engineering

Acknowledgements

I would like to thank Professor Darrell Irvine and Yuhua Hu for all their help and guidance. They were gracious enough to let me be a part of the lab use their resources.

I would like to Eun Chol Cho for his help with some of the data collection for the nanoparticles with different shells

I would also like to thank my family for all their encouragement.

Finally, I would like to thank Tasha Thomas, for all her inspiration and support.

Table of Contents

Abstract	2
Acknowledgements	3
Introduction	6
Experimental Methods	10
Materials.....	10
Synthesis of pH-sensitive core-shell nanoparticles.....	10
Syntheses for reduced particles sizes.....	10
Synthesis of PDEAEMA/PEGMA copolymer nanoparticles.....	11
Synthesis of nanoparticles with different shell compositions.....	12
Synthesis of nanoparticles with shells of different thicknesses.....	12
Dynamic light scattering of particle size distributions and zeta potentials.....	12
Results and Discussion	13
The effect of PAEMA shell on PDEAEMA core pH sensitivity.....	13
The effect of synthesis duration on particle size.....	15
The effect of monomer concentration on particle size.....	21
The effect of a basic synthesis environment on particle size.....	25
Particle stabilization by PDEAEMA/PEGMA Copolymerization.....	27
Synthesis of pH responsive core-shell nanoparticles with different shell compositions.....	32
Conclusions	37

Table of Figures

Figure 1: Schematic of the pH-sensitive core-shell structure and the key chemical ingredients.....7

Figure 2: pH responsive swelling for PDEAEMA cores with and without the PAEMA shell.....14

Figure 3: pH-responsive swelling of PDEAEMA cores with varying synthesis durations.....15

Figure 4: pH-responsive swelling of PDEAEMA cores synthesized with various monomer contents.....23

Figure 5: pH-responsive swelling of PDEAEMA cores synthesized in a basic environment (pH 8).....26

Figure 6: Hydrodynamic diameters of PDEAEMA /PEGMA copolymer nanoparticles synthesized with equal weights of each monomers (0.461 g).....29

Figure 7: DLS measurements of particle size and zeta potentials for the PDEAEMA cores synthesized with different charged shells.....33

Figure 8: pH-responsive zeta potential of nanoparticles with AEMA shells of different thicknesses.....36

Introduction

Several new strategies have been developed that could potentially treat and/or prevent some of the world's most lethal diseases; however, they require the delivery of specific macromolecules into the cytoplasm or nucleus of their target cells. Some of these strategies could involve stimulation of adaptive immunity using synthetic vaccines,¹ tumor suppression using cell-specific toxins,² gene transfection using plasmid DNA,³ and gene silencing using siRNA.⁴ In particular the stimulation of an adaptive immune response is an attractive strategy because it utilizes the body's own defense mechanism and can be applied to both treat and prevent a variety of infectious diseases and even cancer.

One mechanism for the initiation of adaptive immunity involves the uptake of synthetic vaccines or antigens by dendritic cells (DC) because they are antigen-presenting cells that are proficient in activating naïve T cells.⁵ Antigens that reach the DC cytosol are presented much more effectively to CD8+ cytotoxic T cells because they are brought to the cell surface efficiently by the class I major histocompatibility complex molecules.⁶ However, many of the potential drugs and vaccines are membrane-impermeable making it difficult for them to enter the cytosol without being deactivated. Membrane-impermeable macromolecules normally enter the cell via endocytosis, macropinocytosis, or phagocytosis, all of which compartmentalize the macromolecules in closed vesicles, lower the pH, and digest the foreign entity. As a result, there has been significant amount of research investigating potential vectors for the transport of hydrophilic molecules into the cell's cytoplasm.⁷

A promising mechanism for the cytosolic delivery of membrane-impermeable molecules utilized pH-responsive core-shell nanoparticles to disrupt the endosome and disperse the drug throughout the cell.⁸ These vector nanoparticles were synthesized using a two-stage surfactant-free emulsion polymerization; the first stage involves the polymerization of 2-diethylamino ethyl methacrylate

particles with a buffering capacity in addition to the swelling characteristics. To maintain neutrality, chloride ions are transported within the endosome along with the acidifying protons. The PDEAEMA cores within the endosome soak up the influx of protons letting the chloride ions accumulate in the closed vesicle. As a result, the core-shell nanoparticles prevent the adsorbed drug molecules from being denatured by preventing the drop in pH. In addition to the particle swelling, the osmotic swelling due to the chloride accumulation causes the endosome to burst, which is known as the proton sponge effect.⁹ The cytosolic delivery of OVA by the core-shell nanoparticles has also been demonstrated to elicit a functional downstream response in CD8⁺ cytotoxic T cells. After the coincubation of OVA-loaded nanoparticles with bone marrow-derived DCs, cytosolic delivery of OVA was observed in ~ 43% of the cells and a 4-fold increase in naïve CD8⁺ T cell activation compared to controls.

Besides the fact that that the pH-sensitive core-shell nanoparticles facilitated cytosolic delivery of the membrane-impermeable and initiated an adaptive immune response through the activation naïve cytotoxic T cells, this drug delivery system also seems promising because the composition of the shell can be manipulated separately from the endosome-disrupting core to accommodate a variety of different drugs and to target specific cells. In addition, the core-shell nanoparticles have the potential to improve transcutaneous administration of vaccines. Transcutaneous delivery of these core-shell nanoparticles would not only eliminate the need for syringes but would also increase drug efficacy due to the efficient antigen uptake by Langerhan dendritic cells.¹⁰ However, particle penetration into skin is limited by the barrier created by the outermost layer of the epidermis, the stratum corneum. While several strategies have been demonstrated to improve transcutaneous vaccine administration, there have not been any practical transcutaneous vaccines yet. Polylactide-co-glycolide microspheres have been successfully administered transcutaneously using an optimized topical formula that improved particle penetration; however, particle penetration was found to decrease with increasing particle size.¹¹

The pH-responsive core-shell nanoparticles have the potential to facilitate cytosolic delivery of a variety of therapeutic macromolecules, which could improve the effectiveness of transcutaneous vaccines. Our first goal was to synthesize smaller particles so that they could achieve a larger degree of transcutaneous penetration, and our second goal was to synthesize particles with different charged shells to see whether it affects the breadth and types of drugs that could be electrobound. We focused on reducing the diameter of the PDEAEMA core without the PAEMA shell because the core provides the most significant contribution to the core-shell particle size. We tried to reduce the core size by reducing the synthesis duration, reducing the DEAEEMA concentration, decreasing the monomer solubility by increasing the synthesis pH, and sterically stabilizing the particles with an amphiphilic comonomer, poly(ethylene glycol) methacrylate (PEGMA, $MW_{PEO} = 1000$ g/mol). When we reduced the synthesis duration and monomer concentration, we observed smaller PDEAEMA core diameters; however, using the same reaction conditions our particles were typically larger than the previously characterized particles. In order to achieve significantly smaller particle diameters, the small particles most likely require another mechanism for particle stabilization rather than just electrostatic repulsion. To observe whether the shell is actually tunable to provide drug payload flexibility, PDEAEMA cores were synthesized with a polar PEGMA shell, a negatively charged methacrylic acid/PEGMA shell, and a positively charged AEMA/PEGMA shell. In addition, the different charged shells could also affect the endosome-disrupting ability and/or their permeability through the skin. Surprisingly, the particles with the different charged shells all exhibited similar zeta potential measurements, which most likely reflected the surface charge density of the PDEAEMA core. When we synthesized nanoparticles with a smaller PDEAEMA core and a thicker PAEMA shell, we were able to observe a change in the zeta potential that was consistent with the larger positive surface charge density and the higher pK_b of the PAEMA shell. This suggests that the adsorption of positively charged drugs may be difficult because it would require a negatively charged shell that is thick enough to counter the positive PDEAEMA core.

Experimental Methods

Materials

2-diethylamino ethyl methacrylate (DEAEMA, 99%), 2-aminoethyl methacrylate hydrochloride (AEMA, 90%), methacrylic acid (MAA, 99%), and ammonium peroxydisulfate (APS) were purchased from Sigma-Aldrich Chemical Co. Poly(ethylene glycol) dimethacrylate (PEGDMA, MWPEO = 200 g/mol) and poly(ethylene glycol) methacrylate (MWPEO = 1000 g/mol) were purchased from Polysciences Inc.

Synthesis of pH-sensitive core-shell nanoparticles

DEAEMA (1mL, 4.97mmol) and PEGDMA 200 (10 μ L, 0.03mmol) were mixed in an eppendorf tube before being dispersed in 9 ml. The reaction mixture was stirred with a magnetic stir-bar and equilibrated at 70°C for 15min before adding the APS (50 μ L of 200mg/mL freshly made solution) initiator. The synthesis reaction was allowed to run for 3 hrs at 70°C to grow the PDEAEMA particle core. At the end of the 3 hr core synthesis, AEMA (50 μ L of 800mg/mL freshly made solution, 0.24mmol) was injected into reaction mixture to grow the particle shells for an additional 1.5 hrs. The nanoparticles were purified by dialysis (10,000 MWCO Slide-A-Lyzer® Dialysis Cassettes, Pierce Chemical Co.) in 4 L of deionized water for three days followed by three sets of washing by centrifugation (15,000xg for 15 min) and pellet resuspension in PBS (pH 7.4). Purified particles were stored in PBS at 4°C.

Syntheses for reduced particle size

Five different synthesis reactions of PDEAEMA cores were allowed to polymerize for different durations (~3 min, 30 min, 60 min, 90 min, and 180 min). After adding the APS to the reaction mixtures, each sample was maintained at 70°C and stirred for the appropriate period before removing them from

the hotplate. For the ~3 min sample, after adding the initiator, reaction mixture was removed from the hotplate as soon as synthesis reaction turned milky. Once the sample was removed from the heat source, they were immediately injected into a dialysis cassette and placed in a stirred beaker containing 4 L of deionized water.

PDEAEMA cores were synthesized using four different monomer/crosslinker concentrations and otherwise the procedures were the same as those outlined on pg. 5 for the synthesis of the pH-sensitive core-shell nanoparticles except for the addition of the AMEMA shell. The first sample used 1 ml DEAMEA (4.97 mmol) and 10 μ l PEGDMA (0.03 mmol). The second sample used 0.75 ml DEAEEMA (3.73 mmol) and 7.5 μ l PEGDMA (0.023 mmol). The third sample used 0.50 ml DEAEEMA (2.49 mmol) and 5 μ l PEGDMA (0.015 mmol). The fourth sample used 0.25 ml DEAEEMA (1.24 mmol) and 2.5 μ l PEGDMA (0.008 mmol).

For two PDEAEMA core syntheses, 7.5 μ l 1 M NaOH was added to the 9 ml of deionized water prior to the addition of the monomer/crosslinker. The resulting pH was measured to be ~8 using a pH test strip. One reaction was allowed to run for the full 180 min, while the other sample was placed in the dialysis cassette after ~3 min. Otherwise, the reaction conditions were the same conditions for the synthesis of the pH-sensitive core-shell nanoparticles described on pg. 5.

Synthesis of PDEAEMA/PEGMA copolymer nanoparticles

Equal weights of DEAEEMA (0.5 mL) and PEGMA 1000 (0.461 g) were combined in 9 ml deionized water for three synthesis reactions with different SDS surfactant concentrations (No SDS, 20 mg SDS, and 200 mg SDS). No crosslinker was added to any of the three reactions. Otherwise, the we followed the same procedure for the synthesis of the pH-sensitive core-shell nanoparticles.

Syntheses for nanoparticles with different shell compositions

Nanoparticles with three different shells were synthesized (PEGMA , MAA/PEGMA , and AEMA/PEGMA). For each sample, we added an additional 0.5 μl of PEGDMA with the shell, and we used the same total mass for the shell components as we did for the shell in the synthesis of the pH-sensitive core-shell nanoparticles (40 mg). The conditions for the PDEAEMA core synthesis were the same as the synthesis of the pH-sensitive core-shell nanoparticles described on pg. 5. For the PEGMA shell sample, we added 36.36 μl PEGMA 1000 to reaction at the end of the 3 hour core synthesis and allowed the polymerization of the shell to proceed for an additional 1.5 hours. For the MAA/PEGMA and AEMA/PEGMA samples, we used a 2:1 ratio by weight of PEGMA to MAA or AEMA. For the MAA/PEGMA shell we added 24.24 μl PEGMA 1000 and 13.14 μl of MAA. For the AEMA/PEGMA shell, we added 24.24 μl PEGMA 1000 and 13.33 mg AEMA.

Synthesis of Nanoparticles with Shells of Different thicknesses

The thin AEMA shell sample was synthesized following the exact same procedures outlined in the synthesis of the pH-sensitive core-shell nanoparticles on pg. 5. We followed the same procedure for the thicker shell except we used different concentrations for the core/shell monomers, initiator, and crosslinker. To make the core smaller we added only half of the original weights of the reagents used for the core synthesis (0.5 ml DEAEEMA, 5 μl of PEGDMA, and 100 mg APS initiator) to the 9 ml of deionized water. To make the shell thicker we used 4.5x the original weight of AEMA monomer (180 mg) and we added additional crosslinker (2.3 μl PEGDMA).

Dynamic light scattering measurements of particle size distributions and zeta potential

Dynamic light scattering measurements of the particle size distributions were made using 90Plus particle size analyzer from Brookhaven Instruments Corporation. For the instrument parameters we

conducted 6 runs for 30 seconds using a refractive index of 1.5, a dust cutoff of 30, and a 90° scattering angle at 25°C . For sample preparation, $5\ \mu\text{l}$ of the purified nanoparticle suspension was diluted in $150 - 500\ \mu\text{l}$ of appropriate pH 100 mmol PBS buffer so that the concentration was between 100 and 700 kcps. Particle size measurements were repeated for each sample diluting them in each of the different pH 100 mmol PBS buffers (pH 4.83 – 8.17).

For the zeta potential measurements, the zeta potential utilizing phase analysis light scattering (ZetPALS) from Brookhaven Instruments Corporation was used. Because the concentration of our samples was not measured, the particle concentration was assumed to be on the order of $0.01\ \text{mg/ml}$. For sample preparation, $40\ \mu\text{l}$ of purified sample was added to 6 ml of 5 mM NaCl solution. Then the pH of the solution was adjusted using 0.1 M NaOH or 0.1 M HCl to the desired pH. The zeta potential measurements were then repeated for several different pH environments (5.13 – 9.76).

Results and Discussion

The Effect of the PAEMA Shell on the PDEAEMA Core pH Sensitivity

Because the PDEAEMA core is the most significant contributor to the diameter of the core-shell nanoparticles, the PDEAEMA core was the primary target for the reduction in particle size. In order to eliminate the variations in particle size due to the thickness of the PAEMA shell, PDEAEMA cores were mainly synthesized without the addition of the shell. Therefore, the pH sensitivity of the nanoparticles with a PAEMA shell was compared to PDEAEMA core without a shell. Figure 2 shows the hydrodynamic diameters for PDEAEMA nanoparticles with and without the PAEMA shell measured by dynamic light scattering in phosphate buffered saline solutions with pHs ranging from 5.97 to 8.17.

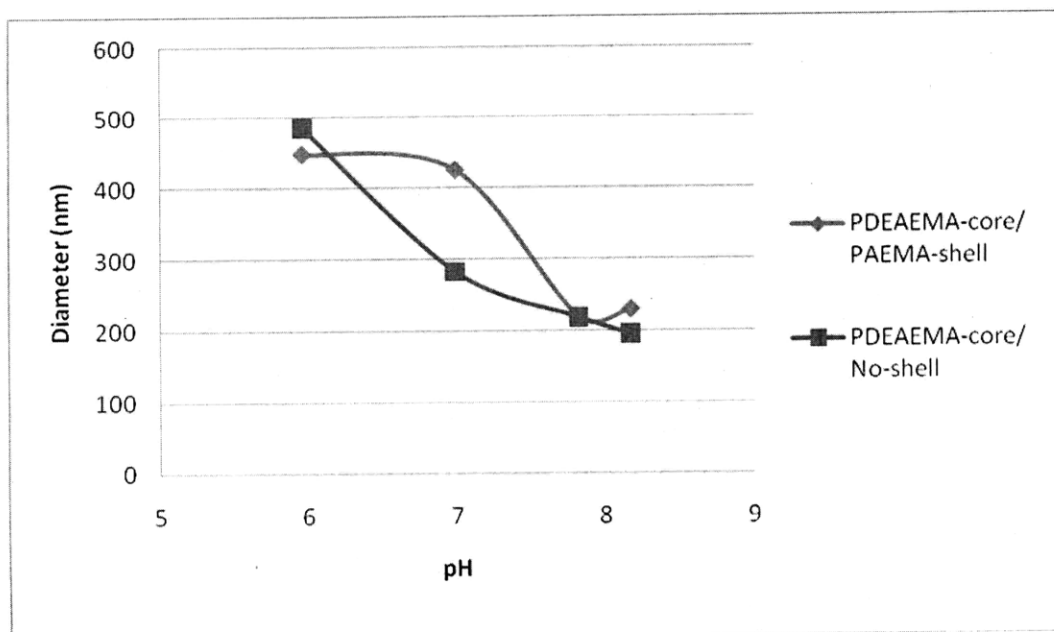


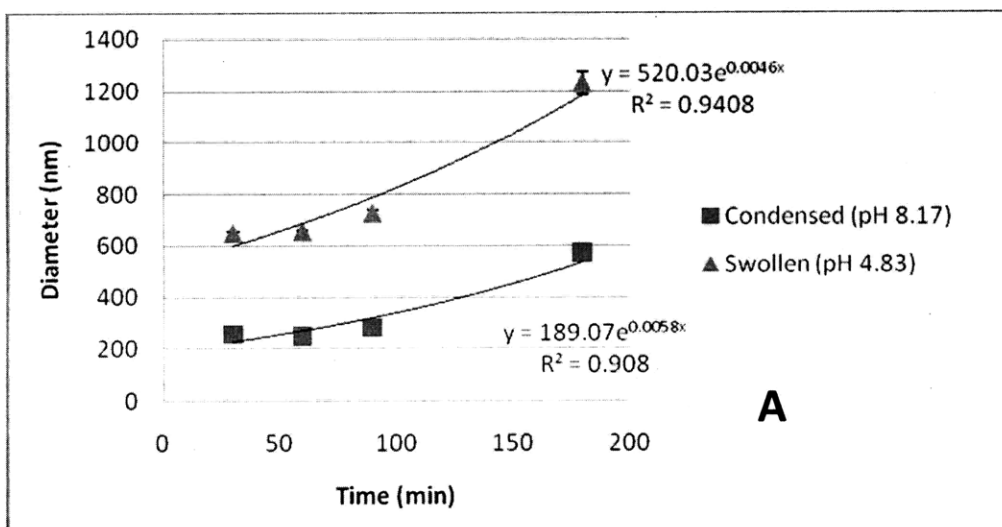
Figure 2. pH responsive swelling for PDEAEMA cores with and without the PAEMA shell. The data points reflect DLS measurements of the hydrodynamic radius for the samples in 100 mmol PBS buffers of various pHs after dialysis and centrifugation washing. The synthesis of the DEAMA cores were the same for both samples. The sample with the shell had 0.24 mmol freshly made AEMA injected after core synthesis and was allowed to grow for an additional 1.5 hours

The presence of the PAEMA shell was not found to alter the measured particle diameter significantly. However, the degree of swelling was observed to be larger for the particles without the PAEMA shell compared to the particles with the shell (2.5 fold increase compared to 2.0 fold increase). These observed pH dependent swellings are comparable to the 2.8 fold increase previously reported for the core-shell nanoparticles synthesized under the same conditions. While the core-shell nanoparticles were previously observed to swell from about 200 nm to 550 nm over the pH range of 9.5 to 4.9, our core-shell nanoparticles swelled from about 230 nm to 450 nm over the pH range of 8.17 to 5.97. The nanoparticles without the shell swelled from 194 nm to 486 nm over the same pH range. The particles lacking the shell could have demonstrated a larger degree of pH sensitivity because they are not constrained by the pH insensitive shell. In addition, the particles lacking the shell also seemed to display the swelling transition at a lower pH. This could be a result of some interaction of the PAEMA shell with the additional protons or experimental error. Nonetheless, for the purposes of this experiment we

determined that the PAEMA core does not significantly affect the particle size across the relevant pHs and that the size of DEAEMA core needed to be reduced in order to produce smaller core-shell nanoparticles.

The Effect of Synthesis Duration on Particle Size

Our first attempt to reduce the diameter of the pH-responsive PDEAEMA cores involved the reduction of the synthesis duration to limit particle growth. After the creation of a polymer phase due to particle nucleation, chain propagation occurs at higher rate within the polymer phase than the aqueous phase (due to the limited solubility of the monomer), which causes the particles to grow over time.¹² By terminating the polymerization reaction at different times subsequent to the start of polymerization, we were able to manipulate the size pH-sensitive PDEAEMA nanoparticles. Figure 3A demonstrates how the PDEAEMA nanoparticle cores that underwent shorter synthesis durations also had smaller hydrodynamic diameters measured by dynamic light scattering. Measurements for each sample were repeated in phosphate buffered saline solutions with pH's varying from 4.83- 8.17 in order to observe the nanoparticles' pH sensitivity.



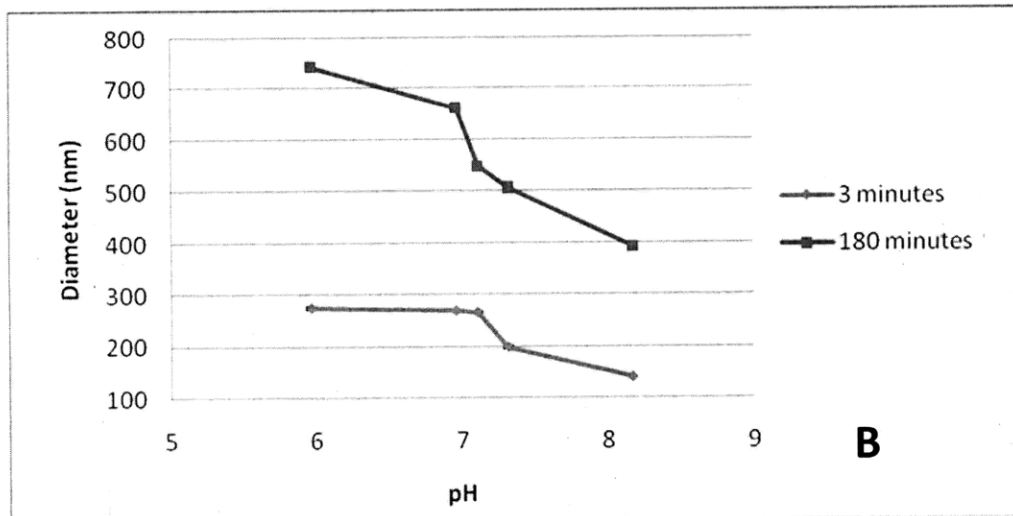


Figure 3. pH-responsive swelling of PDEAEMA cores with varying synthesis durations. (A) Hydrodynamic diameters of syntheses allowed to run for 30 – 180 minutes in 100 mmol PBS buffers with various pHs measured by DLS. (B) Hydrodynamic diameters of syntheses allowed to run for 3 minutes and 180 minutes in 100 mmol PBS buffers with various pHs measured by DLS. Samples underwent dialysis and centrifugation washing prior to DLS measurements.

We observed that the particle size grew exponentially with elapsed synthesis time for each measurement pH (Figure 3A). This trend is not consistent with the findings of Goodall et al. (1977), who reported a parabolic rate law of the form: $(\text{size})^2 = Ct$ for emulsion polymerizations of polystyrene nanoparticles without any added surfactant.¹³ They modeled this growth rate by assuming that the rate limiting event during particle growth was the diffusion of monomer/oligomer into the polymer particles and determined that average number of propagating free radicals within the particles was increasing with particle size. Goodall et al. (1977) setup the polystyrene polymerization reactions using similar conditions (0.870 M styrene, 3.7×10^{-3} M potassium persulfate initiator, 70°C synthesis temperature, no cross-linker); however, rather than stopping the entire reaction, they used large reaction vessels (2 or 4 dm^3) and removed small samples for analysis at various times. In addition, they only measured dehydrated particle sizes using TEM by sampling at least 250 particles. The difference in the observed growth rate could be because of the difference in the polymer system (styrene vs. DEAEEMA), the

different time ranges for particle measurements, or the different procedures for terminating the synthesis reaction.

The difference between the exponential growth rate we observed and the parabolic rate reported by Goodall et al. (1977) was mainly due to the rapid particle growth they observed at small times compared to the slow growth we observed. Although the different reaction kinetics at early time points could be attributed to the different polymerization systems, we believed that the rapid growth rate observed by Goodall et al. (1977) was because they included measurements at smaller times where they could observe primary particles. In our experiment, there was no significant difference between the samples that were allowed to react for 30 and 60 minutes; both demonstrated a 52% decrease in particle diameter on average for all measured pHs compared to samples allowed to run for the full 3 hours (Figure 3A). At pH 8.17 (particles are condensed), the 3 hour synthesis had an average particle diameter of 572.5 ± 7.9 nm with an average polydispersity of 0.123. At the same pH, the 30 minute and 60 minute samples had an average diameter of 257.2 ± 2.9 nm and 248.5 ± 0.4 nm respectively with an average polydispersity of 0.16 and 0.006 respectively. When we repeated the PDEAEMA synthesis for an even shorter time (about 3 minutes), the observed particles were on average 60% smaller for all measured pHs than the particles allowed to run for the full 3 hours (Figure 3B). At pH 8.17, the 3 hour synthesis had an average diameter of 392.4 ± 1.9 nm with an average polydispersity of 0.095. At the same pH, the 3 minute synthesis had an average diameter of 141.2 ± 0.9 nm with an average polydispersity of 0.004. It should be noted that the 3 hour control synthesis in Figure 3b produced particles that were on average 37% smaller for all measured pHs than the particles produced by the 3 hour synthesis in Figure 3A. In addition, we could not identify any clear trend when comparing the polydispersity of the particles versus time; all the synthesized particles were found to be monodisperse with a polydispersity less than 0.2 measured by DLS (data not shown). However, it should be noted that DLS is not considered to provide reliable polydispersity measurements.¹⁴ Although the 3 minute

synthesis was comparable to the duration where Goodall et al. (1977) and others reported to have observed primary particles, we were not able to observe a significant decrease in particle size associated with primary particles compared to the 30 minute and 60 minute syntheses. We believe that we did not observe significantly smaller particles after the 3 minute synthesis because primary particles are colloidally unstable, which makes them susceptible to coagulation. The coagulation of smaller particles could also explain why there was not much of a difference between the sizes of the particles that ran for 30 min compared to the particles that ran for 60 min.

Assuming that we were not able to measure primary PDEAEMA particles, we compared our procedure for terminating the synthesis reactions to the procedure employed by Goodall et al. (1977) in order to determine why we were unable to prevent coagulation. After experiencing some difficulties using hydroquinone to inhibit polymerization, Goodall et al. (1977) adopted a technique in which they immediately diluted the sample (1:100) and stored them at 15^o C. With these conditions, they claimed to have observed 5-10 nm or larger primary particles after about 5 minutes, which rapidly increased in size and became monodisperse after about 30 minutes. We followed a similar procedure. Because we conducted smaller scale synthesis reactions, we removed the entire sample from the heat source and transferred the turbid solution into a dialysis cassette to be placed in about 3 liters of MilliQ deionized water at room temperature (about 25^o C) after the desired synthesis period. Our particles could have coagulated because we did not dilute the samples immediately after removing them from the heat source or because we did not store them in a cold enough environment. In addition, thermal termination of the polymerization reaction might not provide a precise method for identifying the small initial particles. By cooling the samples, we reduce or eliminate the decomposition of initiator into free radicals, but this does not eliminate the free radicals that already exist throughout the system. After the samples have been removed from the heat source, there may be some additional time for polymerization before the free radicals terminate in the aqueous or polymer phases. In addition, there

could also be some residual initiator decomposition after the samples are removed from the heat source due to variations associated with the cooling rate of the samples. However, we believe that the most likely cause of particle coagulation was the conditions for centrifugation washing. Small particles could be colloidally stable because we used an amphiphilic crosslinker, some of the chains ends could possess a de-protonated sulfate group from the initiator at the particle surface, and the DEAEMA cores themselves possess a tertiary amine with pK_b of 7.0-7.3 (some of which would be protonated because the reaction takes place in deionized water with $pH \sim 5$ prior to the addition reagents). According to DLVO theory, which takes into consideration the potential energy of any two mutually approaching particles due to van der Waals and electrical double layer interactions, the potential energy barrier of these charged particles could be enough to stabilize the particles from aggregating due to Brownian motion. This potential energy barrier depends on the concentration and nature of the electrolyte environment, the particle size, and the surface-charge density.¹⁵ Therefore, the centrifugation washing process provides a serious threat to the colloidal stability of small particles. Following the procedure for nanoparticle preparation described by Hu et al. (2007), we centrifuged the synthesis products 3 times at 15,000xg with PBS (pH 7.4) to remove any unused long polymer chains that could not be removed by the 10,000 MWCO dialysis cassettes. The centrifugation was conducted using 100mmol PBS (pH 7.4) in order to mimic physiological conditions because of the potential drug-delivery applications. This process was deemed necessary in order to remove the excess polymer chains that would potentially interfere with DLS size measurements. However, the 100 mmol PBS solution provided an electrolyte environment that could have diminished the potential energy barrier keeping the small particles isolated and the centrifugation could have compacted the particles into a pellet forcing the particles to a much closer proximity. As a result, we should either repeat these experiments without the centrifugation washing step or at least try washing with deionized water as this process greatly increases the chances of coagulation. In addition, the DLS size measurements using basic PBS buffers could also promote

coagulation of smaller particles. The pK_b of the tertiary amine in the PDEAEMA core is 7.0 – 7.3; therefore, the DLS measurements for the condensed particles at basic pHs reduce the degree of ionization of the DEAEMA monomers, which, in turn, decreases the zeta potential. The reduced electrostatic repulsion between neighboring would greatly increase the chance for particle coagulation due to Brownian motion.

We also observed variations in the sizes measured for the particles created using the previously established reaction conditions. The 180 minute synthesis samples were synthesized and measured by DLS following the experimental procedures described by Hu et al. (2007) (except for the additional polymerization step for the AEMA shell); however, in Figure 3A, our particles measured twice as large over the same pH range. For the full 3 hour synthesis, Hu et al. (2007) reported a diameter of around 210 nm determined by DLS at 25 °C in PBS buffer with pH 8.07 and physiological ionic strength. Following the same procedures, our particles were found to have average diameter of 572.5 ± 7.9 nm (Figure 3A) and 392.4 ± 1.9 nm (Figure 3B) when the reaction was allowed to run for the full 3 hour period. These differences could be attributed to procedural errors. For example, hydrophobic monomer droplets were kept dispersed in the deionized water by stirring using small cylindrical magnetic stir bars. Some stir bars were found to have more stable rotations than others at the rotation speed required to disperse the monomer droplets. In particular, some of the stir bars could not be maintained so that they only rotated about one axis; some would revolve around the bottom of the 15 ml vial as they rotated. As a result, the variable mixing conditions also could have contributed to the variations observed for repetitions of the synthesis reactions with the same setup conditions. In addition, both procedures did not include the deionized water containing the monomer and crosslinker being sparged with nitrogen prior to the addition of the initiator. When we attempted to sparge the samples, the tubing that would bubble the nitrogen would prevent us from establishing stable rotations for some of the stir bars that kept the monomer dispersed. Because the samples were not provided

with an inert environment, daily differences in atmospheric pressure and humidity could produce variations in the concentration of oxygen within the synthesis environment, which would produce variations in the amount of free radical termination. We decided that variation in particle size due to poor stirring was more significant than the variations due to atmospheric oxygen fluctuation and radical termination.

The Effect of Monomer Concentration on Particle Size

Because the rate of particle nucleation and particle growth have both been found to depend on monomer concentration, we decided to see if we could decrease the particle size by reducing the monomer concentration.^{16,17} The Fitch-Tsai equation provides a qualitative tool for understanding the key processes that determine the rate of nucleation in emulsion polymerization:¹⁶

$$\left(\frac{dN}{dt}\right) = bR_{iw} - R_c - R_f \quad (1)$$

where N is the number of particles per liter (dm^{-3}), R_{iw} is the rate of chain initiation in the aqueous phase, b is scaling factor that takes into account the fact that not all radicals lead to propagation due to side reactions, R_c is the overall average rate of oligoradical capture by particles, and R_f is the overall average rate of coagulation.¹⁶ The particle nucleation rate has a strong dependence on monomer concentration because R_{iw} depends on the concentration of monomers available for chain initiation and R_c depends on the concentration of oligomeric radicals (which also depends on the concentration of aqueous monomers) that can be captured by the particles for particle growth. The nucleation rate becomes important in determining the particle size because there is limited amount of radicals and monomer. Conservation of mass dictates that the greater the number concentration of nucleated particles, the smaller the monomer concentration in the polymer phase; thus, larger nucleation rates

tend to produce smaller particles.^{16,18} However, the particle coagulation rate provides an additional competing process that also governs particle size. Verwy and Overbeek (1948) created a model for the particle coagulation based on Smoluchowski and Fuchs' and DLVO theories in which the particle coagulation rate depends on the square of the number concentration of particles. Finally, the monomer concentration also affects the particle size distribution because it governs particle growth after nucleation. Growth from the propagation of polymer chains within the particles depends on the concentration of monomers and the concentration of propagating radicals within the polymer particles. In light of these competing processes that determine particle size, we found that the particle size decreased with decreasing monomer concentrations. Figure 4 demonstrates how the hydrodynamic diameters of PDEAEMA nanoparticle cores measured by dynamic light scattering decreased with decreasing total initial monomer concentration. The control sample (4.97 mmol DEAEMA, 0.03 mmol PEGDMA) was synthesized following the protocol described by Hu et al. (2007) except for the addition of AEMA shell. Parallel PDEAEMA core synthesis reactions were conducted in following the same procedure except the initial monomer and cross-linker concentrations were decreased. In each synthesis, the molar percent of crosslinker to monomer was maintained at 0.6% in order to eliminate any variation in particle diameter due to the degree of crosslinking. Measurements for each sample were repeated in phosphate buffered saline solutions with pH's varying from 6.96- 7.82 in order to demonstrate that the nanoparticles still maintained their pH sensitivity.

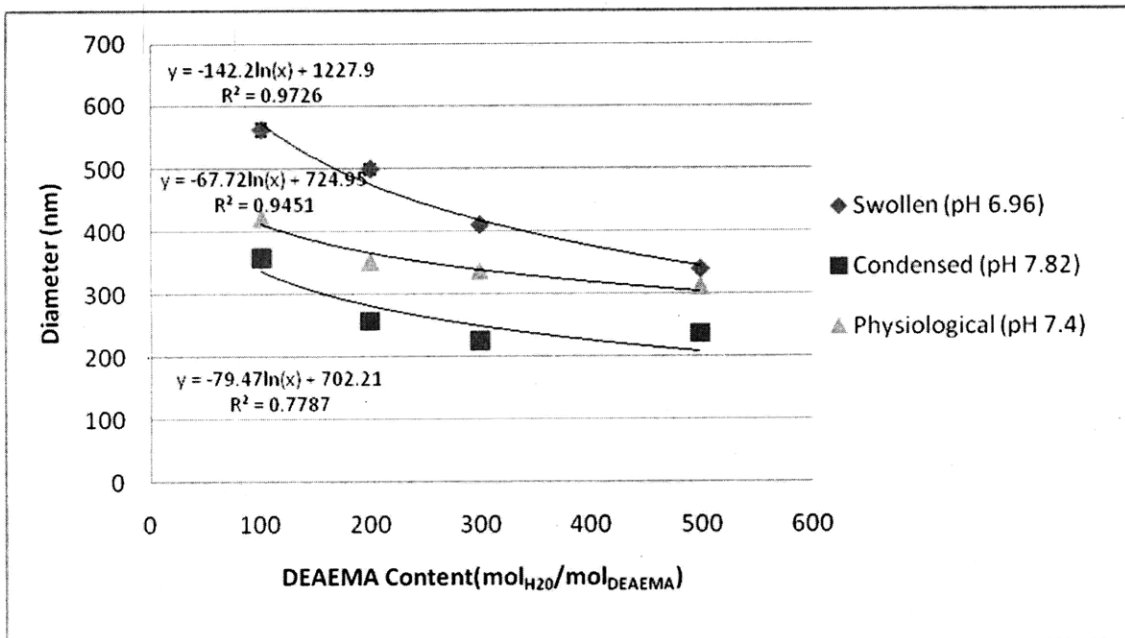


Figure 4. pH-responsive swelling of PDEAEMA cores synthesized with various monomer contents. Hydrodynamic diameters in 100 mmol PBS buffers with various pHs measured by DLS. Monomer:Crosslinker molar ratio was maintained for each sample. Each sample had 0.04 mmol APS.

We observed a logarithmic dependence between monomer content ($\text{mol}_{\text{H}_2\text{O}}/\text{mol}_{\text{DEAEAMA}}$) and the hydrodynamic radius of the synthesized PDEAEMA core nanoparticles. This observation is consistent with the linear decrease in hydrodynamic particle diameter observed by Wutzel and Samhaber (2007) when they decreased the initial concentration of styrene monomer in the emulsion polymerization of polystyrene nanoparticles using SDS as a surfactant.¹⁹ It should be noted that because Wutzel and Samhaber (2007) a surfactant, they observed a constant particle number concentration with varying monomer content; therefore, they attributed the decrease in size to the decreased supply of monomer from the droplets to the initiated micelles. Although we did not use a surfactant, the PEGDMA crosslinker is amphiphilic and could form micelles to initiate polymer particles. We did not measure the particle number concentration for our synthesis reactions, but the similar trend for particle size versus monomer content suggests that the initial monomer content might not have a significant effect on the particle number concentration for our surfactant-free system. Because all of our particles were found to

be monodisperse by DLS (data not show), this suggests that the initial period for stable particle formation should be small.¹⁶ Therefore, it is conceivable that the particle number concentration would not change significantly with varying initial monomer content if instead the initial rate of particle nucleation depends on the solubility of the monomer (which governs $[M]_w$) and the initiator concentration (which remained constant).

We observed an 32% average decrease across the entire pH range (6.96 – 7.82) for the nanoparticles synthesized using a 5-fold decrease in monomer content (1.00 mmol DEAEMA and 7.5×10^{-3} mmol PEGDMA) compared to the nanoparticles synthesized following the protocol reported by Hu et al. (2007), which used 4.97 mmol DEAEMA and 0.03 mmol PEGDMA. When the particles were measured in 100 mmol PBS pH 6.96, our particles synthesized following Hu et al. (2007)'s protocol had a hydrodynamic diameter of 561.7 ± 10.1 nm while the particles synthesized using a 5-fold decrease in monomer content had a hydrodynamic diameter of 339.9 ± 1.9 nm measured by DLS. Using the same synthesis conditions, our particle sizes were larger again compared to those previously reported by Hu et al. (2007) at the same pH, and the particles synthesized with the 5-fold decrease in monomer content were 32% smaller. However, our particles exhibited a smaller degree of condensation when placed in a basic environment (pH 7.82). At this pH, our particles synthesized following Hu et al. (2007)'s protocol had a hydrodynamic diameter of 358.2 ± 2.7 nm while particles synthesized using a 5-fold decrease in monomer content had a hydrodynamic diameter of 236.1 ± 3.2 nm. Compared to the ~ 2.4 -fold change in diameter reported by Hu et al. (2007) over the pH range 7.0 – 8.0, our particles synthesized under the same conditions and the particles synthesized with the 5-fold decrease in monomer content exhibited a 1.6 and 1.4 change in diameter respectively over the pH range 6.96 – 7.82. The day to day variations in hydrodynamic radius between experiments for the particles synthesized under the same conditions were larger than the observed decrease in swelling; therefore, the observed decrease in diameter could be a result of the procedural errors discussed above in the experiment with varying synthesis durations.

The Effect of a Basic Synthesis Environment on Particle Size

Because the rate of particle nucleation and thus the particle number concentration depends on the concentration of monomer in the aqueous phase, we wanted to see if we could reduce the particle size by decreasing the DEAEMA solubility using a basic synthesis environment. The pH of the deionized water previously used for particle synthesis had a pH of ~ 5 . At this pH, almost all of the tertiary amines of the DEAEMA monomer (pK_b of 7.0 – 7.3) would be protonated; therefore, we chose to conduct a synthesis in which we adjusted the pH of deionized water to a higher pH to reduce the amount of protonated DEAEMA monomers. After adding the monomer and crosslinker to the deionized water, the pH for the reaction mixture was measured to be 9.38, which suggests that the DEAEMA monomers already absorbed a significant amount of H^+ ions from the aqueous environment. Therefore, we decided to adjust the pH of the aqueous reaction environment to pH 8 using 7.5 μ l 1 M NaOH prior to the addition of monomer and crosslinker. Figure 5 shows the hydrodynamic diameters of the particles synthesized in the basic environment for 180 minutes and 3 minutes measured by DLS in 100 mmol PBS buffers from pH 5.97 to pH 8.17.

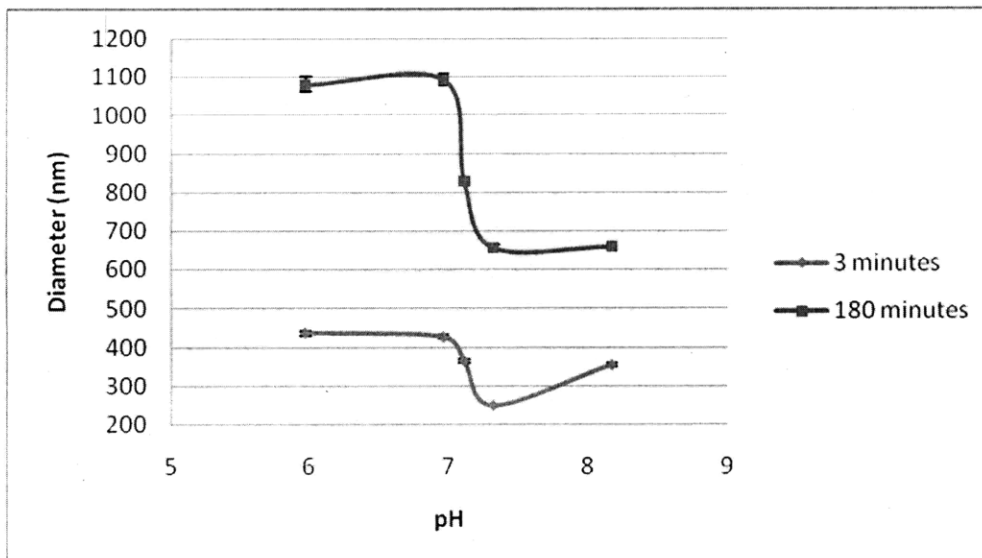


Figure 5. pH-responsive swelling of PDEAEMA cores synthesized in a basic environment (pH 8). 7.5 ul of 1 M NaOH was added to the water prior to the addition of monomers. Hydrodynamic diameters were measured in 100 mmol PBS buffers with various pHs by DLS.

The 3 minute samples were on average 57% smaller than the 180 minute samples across the entire pH range, which is consistent with our findings in the synthesis duration experiment (Figure 3B); however, the particles synthesized in the pH 8 aqueous environment had larger measured hydrodynamic diameters. Particles synthesized in the basic environment were 36% larger for the 180 minute samples and 34% larger for the 3 minute samples compared to the particles from the synthesis duration experiment in Figure 3B. The larger particles were most likely a result of the decreased monomer solubility in the aqueous phase. Because the nucleation rate depends on the concentration of monomer in the aqueous phase, the decreased monomer solubility would most likely decrease the initial particle number concentration. This trend would still hold true regardless of the mechanism for particle nucleation (i.e. precipitation of critical length polymer chain, particle growth in surface active oligomeric radical micelles, or particle growth in amphiphilic PEGDMA micelles). Decreasing the particle number concentration could lead to a larger distribution of particle sizes due to the fact that there

would be a larger concentration of available monomers per particle.¹⁶ This becomes significant when you consider that the radicals and monomer have to cross the particle/water interface.¹⁸ In addition, decreasing the monomer solubility in the aqueous solution could increase the monomer concentration in the polymer phase. In support of this hypothesis, Ceska (1974) found that increasing hydrophobicity of carboxylic monomer used in the surfactant free emulsion copolymerization of polystyrene nanoparticles increased the nucleation rate and the number concentration of particles.²⁰ They demonstrated that the more hydrophobic carboxylic monomers diffused more rapidly to particle surface stabilizing the particles against coagulation.²⁰ Therefore, increasing hydrophobicity of the DEAEMA monomer could increase monomer diffusion to the polymer particles, which would increase the rate of particle growth. However, the diameters of the particles synthesized for 3 hours in the basic environment were only slightly smaller than the particles synthesized for 3 hours under normal conditions. This suggests that the increased size of the particles from the basic synthesis could be a result of the procedural errors noted in the synthesis duration discussion section.

Particle Stabilization by PEGMA/DEAEMA Copolymerization

The surfactant-free aspect of the emulsion polymerization system reported by Hu et al. (2007) has several advantages for the potential drug chaperone applications of the core-shell nanoparticles. The addition of a surfactant to the emulsion process would hinder their industrial viability because of the potential toxicity of common surfactants and the difficulties associated with their removal.²¹

Nonetheless, we decided to conduct PDEAEMA emulsion polymerization with surfactant due to the previous unsuccessful attempts to reduce particles size. Surfactant facilitated emulsion polymerization commonly produces smaller particles because there surfactant micelles can capture initiated oligomer radicals to form new particles at a faster rate and for longer periods. The increased number concentration of surfactant stabilized particles leads to smaller sizes. Unsurprisingly, the particles

synthesized with two different SDS surfactant concentrations (0.2 and 2 wt% of the total synthesis reaction) and various synthesis conditions all precipitated upon purification by dialysis. Although the additional stabilization provided by the SDS may have led to the synthesis of smaller particles, the particles could not remain stable when the SDS was removed by dialysis, and the particles coagulated to form a bulk polymer phase. Upon observing this phenomenon, we decided to try a different mechanism for particle stabilization that utilized the increase in interfacial free energy associated with surfactant removal. Using surfactant emulsion copolymerization of DEAEMA/PEGMA 1000, we hoped to produce long polymer chains with equal mole fractions of DEAEMA and PEGMA monomers (randomly oriented) that were water soluble due to SDS surface stabilization. Upon the removal of the surfactant, we hypothesized that the chains would collapse to conceal the hydrophobic DEAEMA units with the hydrophilic PEGMA counterparts producing polymer brush stabilized nanoparticles. Figure 6 shows the hydrodynamic diameters of the DEAEMA/PEGMA nanoparticles formed without any crosslinker using two different SDS concentrations (0.2 and 2 wt% of total synthesis reaction). The hydrodynamic diameters were measured by DLS twice: once in 100 mmol PBS buffer pH 7.4 and then again after the addition of 1 M NaOH to raise the pH to ~ 9.

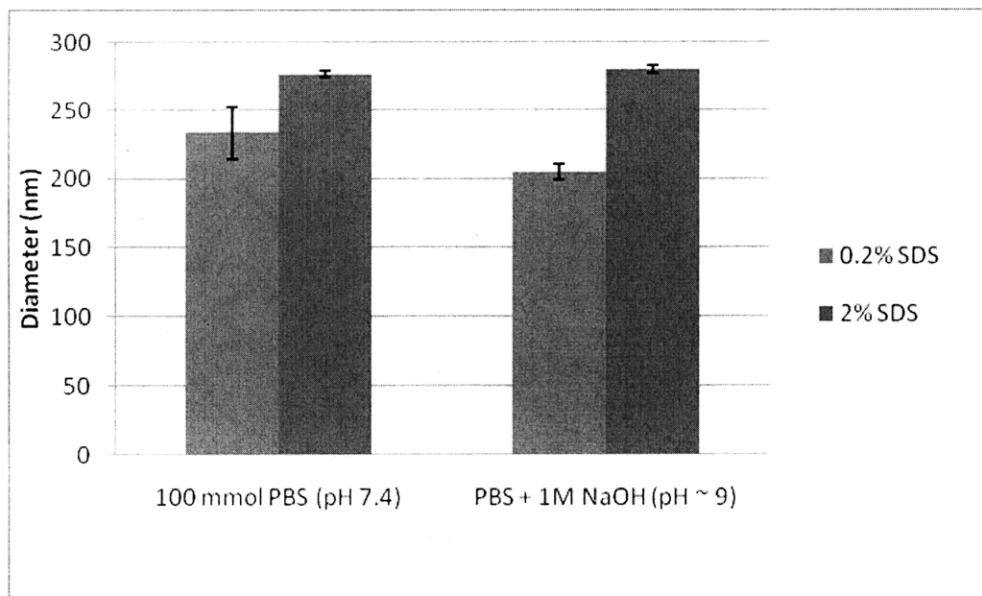


Figure 6. Hydrodynamic diameters of PDEAEMA /PEGMA copolymer nanoparticles synthesized with equal weights of each monomers (0.461 g). Because of the small total volume of synthesized nanoparticles, the particles were measured in the 100 mmol PBS buffers at pH 7.4 used for the centrifugation washing. The measurement was then repeated after adjusting the pH to ~9 using 1 M NaOH.

Without any added surfactant, no copolymer nanoparticles were formed because the lack of surface stabilization led to coagulation and precipitation. Interestingly, there was no change in particle diameter for DEAEMA/PEGMA nanoparticles synthesized with a 2 wt% SDS concentration. This is most likely because these nanoparticles contained a significantly smaller mole fraction of DEAEMA monomers compared PEGMA monomers. This hypothesis seems reasonable because both the PEGMA monomers and initiator are water soluble compared to the barely water soluble DEAEMA monomers; therefore the PEGMA monomers most likely have a much larger polymerization rate. On the other hand, the DEAEMA/PEGMA nanoparticles synthesized with a 0.2 wt% SDS concentration were smaller than those synthesized with the larger SDS concentration and exhibited a 12% decrease in diameter when the pH was increased from 7.4 to 9. The limited pH sensitivity of these particles suggests that they have a larger mole fraction of DEAEMA monomers than the mole the particles synthesized with the higher SDS

concentration. The surfactant concentration could alter the DEAEMA mole fraction in the copolymer nanoparticles because a significant change in surfactant concentration could change the polymerization rates for each monomer or even the primary locus for polymerization. The diameters for the 0.2 wt% DEAEMA/PEGMA sample are slightly smaller than those observed by Hu et al. (2007) over the same pH range.

It is important to note that the synthesis of the DEAEMA/PEGMA nanoparticles was not as efficient as synthesis of the crosslinked DEAEMA nanoparticles in terms of the total volume of synthesized nanoparticles. Using the same mass of DEAEMA monomers and the same synthesis duration, the volume of the DEAEMA/PEGMA nanoparticle pellet was much smaller during the centrifugation wash. The pellet volume was so much smaller that a different procedure was used in order to measure the pH-sensitivity of the particles using DLS. The DEAEMA/PEGMA particle number concentration was so small that dilution with the different pH PBS buffers decreased the DLS count rate below the critical level for reliable size measurements. The steric stabilization provided by the polymer brush structure of the PEGMA at the particle interface is could facilitate the creation of smaller, pH-sensitive particles by decreasing the molecular weight of the surfactant stabilized chain. Future experiments would include manipulating the reaction kinetics (i.e. synthesis time, monomer concentration, initiator concentration etc.) and varying the proportions of DEAEMA and PEGMA monomers to create lower molecular weight.

The results of the experiments in which we attempted to reduce the particle size suggest that the manipulation of the polymerization kinetics is not the most practical method for obtaining significantly smaller particles. Smaller particles obtained in this fashion are less stable because of their reduced charge density, and they have no other mechanism to prevent coagulation except for electrostatic repulsion. One future study would include reducing the monomer to crosslinker ratio; however, this would not provide any additional stabilization for smaller particles, which would leave

them susceptible to coagulation. We could increase the initiator concentration; however this would most likely not significantly reduce the particle size. The increase in the rate of nucleation and the particle number concentration generally leads to smaller particles, but the increased number of particles would also increase the rate of coagulation. In addition, a larger initiator concentration would also increase particle growth because of the increase in the polymerization rate, and the additional deprotonated sulfate groups at the chain ends would not help stabilize the particles because they're negatively charged. We could also try to use the PAEMA shell to stabilize smaller particles because it would remain charged due to its high pK_b ; however, we would have to be careful not to add the shell too early during the core synthesis because this could lead to a bimodal distribution from the synthesis of PAEMA rich particles. Although we only tried SDS for the surfactant, other surfactants would most likely fail to reduce the particle size because they would also be removed during dialysis, which could lead to coagulation or precipitation. Even if we successfully synthesized smaller electrostatically stabilized particles, the purification by centrifugation and the DLS measurements in the basic PBS buffers would most likely cause them to become colloidal unstable, unless we provide the particles with an alternative stabilization mechanism like steric stabilization. Manipulation of the polymerization kinetics and the relative monomer fractions for PDEAEMA/PEGMA copolymer particles could be successful in reducing the particle size; however, the polymer brush stabilizing the surface could interfere with electrostatic drug binding. Additional mechanisms for the stabilization of small particles need to be explored. Once we successfully synthesized significantly smaller molecules, future studies would include measuring the drug binding capacity using fluorescent OVA, and incubating DC cell cultures with cy5-labeled nanoparticles loaded with fluorescent OVA to compare the endosome-disrupting ability of the smaller particles to those observed by Hu et al. (2007).

Synthesis of pH-Responsive Core-Shell Nanoparticles with Different Shell Compositions

Because the primary mechanism for loading drugs on the core-shell nanoparticles characterized by Hu et al. (2007) is electrostatic adsorption, the particle surface charge governs the type, amount, and release of the drugs that can be adsorbed. In particular, the PAEMA shell used by Hu et al. (2007) remains positively charged across the pH range required for drug delivery, which would only adsorb negatively charged drugs. Therefore, we wanted to synthesize core-shell nanoparticles using monomers that would produce different charged shells to see whether this system could be manipulated for the delivery of a wider variety of drugs. We created nanoparticles with three different shells: a positively charged PAEMA/PEGMA shell, a negatively charged MAA/PEGMA shell, and a polar shell with just PEGMA. Compared to the core-shell nanoparticles created by Hu et al. (2007), we used the same procedure for PDEAEMA core synthesis, the same total mass of shell monomer, and the same shell synthesis duration; however, we maintained a 2:1 (PEGMA:Charged Monomer) ratio by mass for the positively and negatively charged shells and added additional crosslinker. Figure 7 shows the size and zeta potential measurements using DLS for the core-shell particles with the different charged shells.

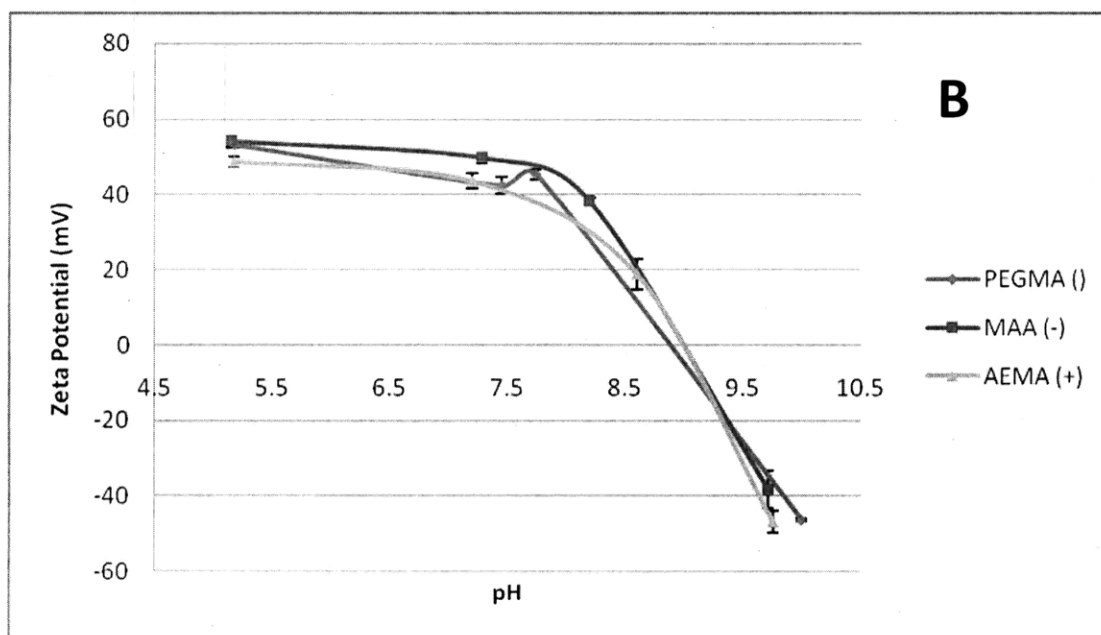
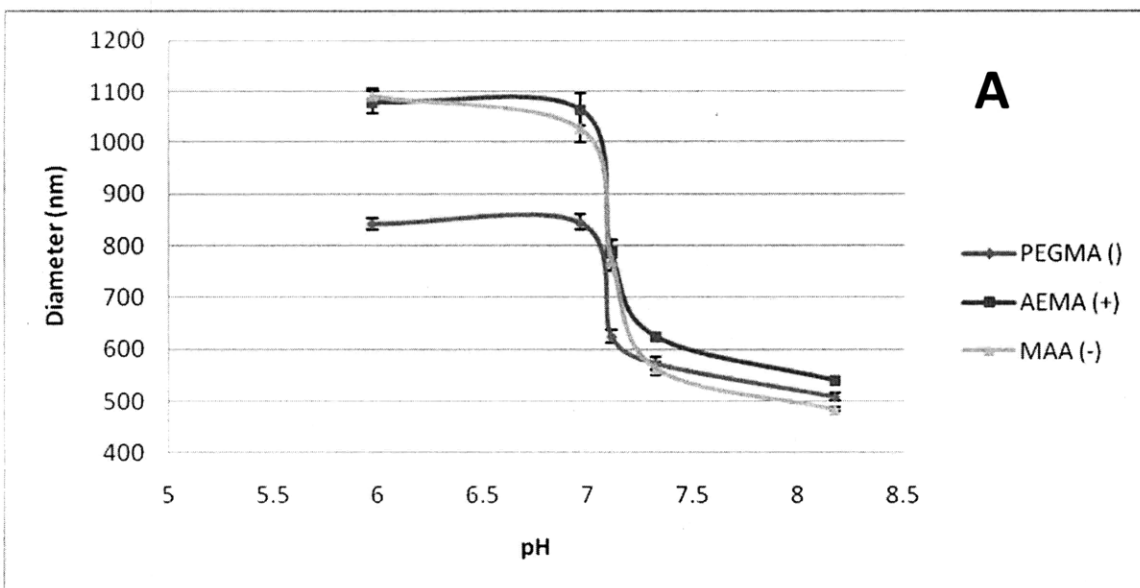


Figure 7. DLS measurements of particle size and zeta potentials for the PDEAEMA cores synthesized with different charged shells. (A) Hydrodynamic diameters of nanoparticles with different shells measured by DLS in 100 mmol PBS buffers at various pHs. (B) Zeta potential was measured for the nanoparticles with different shell using DLS in 5 mM NaCl solutions with various pHs adjusted by 1 M NaOH and 1 M HCl.

The nanoparticles with PAEMA/PEGMA and MAA/PEGMA shells were about twice the size of those reported Hu et al. (2007) across the same pH range. In addition we observed a smaller change in particle diameter (1.65 for the PEGMA shell particles, 1.99 for PAEMA/PEGMA shell particles, and 2.26 for the PMAA/PEGMA shell particles). The increased size and decreased swelling could be the result of the additional crosslinker added during the shell synthesis. The additional PEGDMA could have increased the amount of crosslinked chains, which might increase the number of core/shell chains per particle and decrease the separation between chains during particle swelling. Alternatively, the diameters for the particles with the PAEMA/PEGMA and MAA/PEGMA shells were also similar to the diameters measured for 3 hour samples in the synthesis duration and basic synthesis environment experiments (Figure 3A and Figure 5). The consistent size difference between our particles suggests that there could just be a systematic error in the way we reproduced Hu et al. (2007)'s nanoparticle synthesis.

Interestingly, the particles with the PEGMA shell had a similar diameter to the particles with the PAEMA/PEGMA and MAA/PEGMA shells in the condensed state at pH 8.17; however, in the swollen state at pH 5.97, the PEGMA shell particles were an average of 22% smaller between both the populations of particles with charged shells. Although PEGMA was added during the synthesis of each shell type, the decreased swelling for the particles with only the PEGMA shell could be because of the increased chain interpenetration and/or increased crosslinking between chains. Because the PEGMA monomers are amphiphilic, they can most likely penetrate deeper into the hydrophobic PDEAEMA cores than the charged shell monomers. Because we also added extra crosslinker during the shell synthesis, the crosslinking PEGMA chains deeper within the particles could limit the degree of swelling.

The zeta potentials were measured by DLS in 5 mM NaCl solutions with various pHs and were nearly identical for each of the nanoparticles even though their shells had different charges (Figure 7B). The zeta potentials changed from about +50 mv to about -50 mv across a pH range of 5 – 10 with an

isoelectric point at about pH 9 for each sample. If we assume that we were successful in polymerizing the nanoparticles with shells of different charges, then this suggests that the shells have an insignificant effect on the distribution of ions surrounding the particle surface. This would imply that the zeta-potential measured for each sample reflects the charge density of the inner PDEAEMA core instead of the different shell layers, which seems reasonable when you consider how the PDEAEMA core comprises such a larger volume compared to the thin shell layers. The isoelectric point at pH 9 suggests that the observed zeta potentials reflect the PDEAEMA core because at that pH we would expect nearly all of the tertiary amines from the DEAEMA monomer (pK_b 7.0-7.3) to be uncharged. An important consequence from this observation is that the addition of the MAA/PEGMA shell probably would not allow the core-shell nanoparticles to adsorb positively charged drugs.

To test the hypothesis that the shells had no affect on the zeta potential due to the relative sizes of the cores and shells, we synthesized another set of nanoparticles in which we attempted to reduce the size of the PDEAEMA core and increase the thickness of the PAEMA shell. To reduce the core thickness, we used half the weight of the DEAEMA monomer, PEGDMA crosslinker, and APS initiator compared to the amounts used by Hu et al. (2007), and we let the synthesis run for only 1 hour. For a thicker shell, we added 4.5x the normal weight of AEMA with 0.5 mol% of PEGDMA. Figure 8 shows the zeta potentials measured using DLS in in 5 mM NaCl solutions with varying pHs for the particles with different PAEMA shell thicknesses.

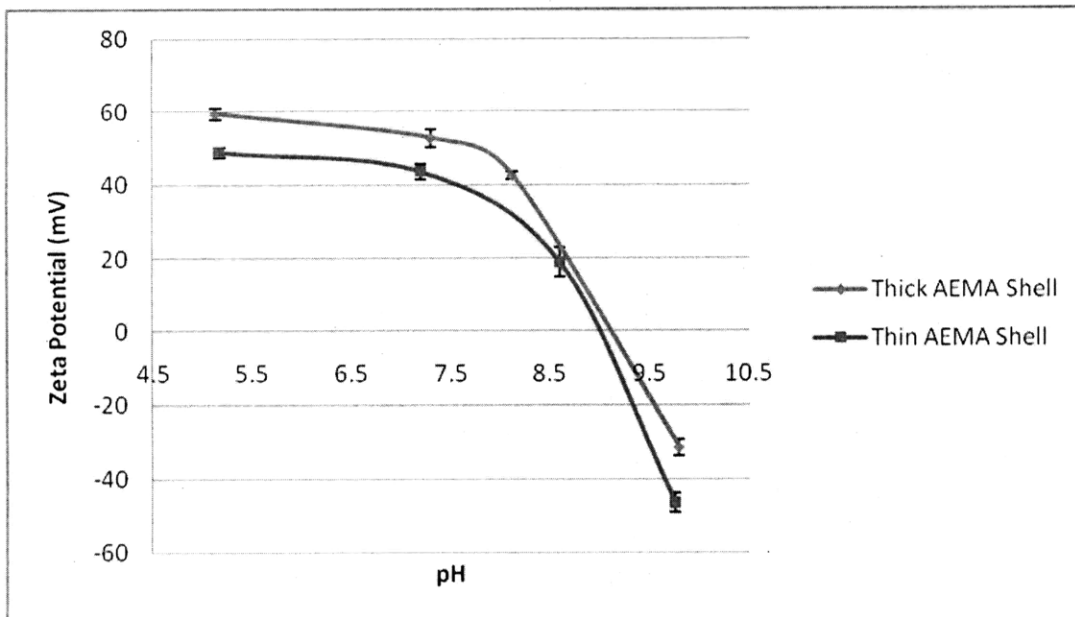


Figure 8. pH-responsive zeta potential of nanoparticles with AEMA shells of different thicknesses. The thick AEMA shell particles were synthesized using half the reagent concentrations for the PDEAEMA core and 4.5 x the weight of AEMA (180 mg) synthesized. Zeta potential was measured using DLS in 5 mM NaCl solutions with various pHs adjusted by 1 M NaOH and 1 M HCl.

Although we did not confirm that the relative thickness of the cores and shells were actually changed, we did observe an increase in the maximum zeta potential and the isoelectric point for the particles with the thicker PAEMA shell compared to the particles synthesized following Hu et al. (2007)'s procedures. The maximum zeta potential was 60 mV and the isoelectric point was at ~ pH 10 for the particles with thicker shells. The shift toward a larger positive zeta potential and a higher pH isoelectric point is consistent with an increase in the relative amount of PAEMA compared to PDEAEMA. The zeta potential most likely increased at the acidic pH because the PAEMA does not exhibit pH dependent swelling; therefore, PAEMA maintains a higher positive charge density in acidic environments compared to the PDEAEMA. The higher pH isoelectric point is most likely due to the increase in the relative amount of the primary amines ($pK_b \sim 11$) in the AEMA monomer, which remain charged at higher pHs

compared to the DEAEEMA monomers. These observations support our hypothesis that we couldn't observe any changes in the potentials from the different shell charges because we synthesized relatively thin shells. The adsorption of positively charged drugs on a negatively charged shell still doesn't look promising because the negative shell would have to be thick enough to overcome the positive charge associated with the PDEAEMA core.

Future studies would include measuring the drug binding capacity of the particles with the different charged shells with different thicknesses to see if there is any difference in the amount of fluorescent OVA that binds to the particles. In addition, cell culture experiments involving incubation of DCs with calcein and the particles with different shells to see if the different shell charges affects the endosome-disrupting capacity of the nanoparticles.

Conclusion

The pH-responsive PDEAEMA-core/PAEMA-shell nanoparticles have the potential to be a powerful tool in the development of new treatments for a variety of diseases. In particular, their ability to facilitate efficient cytosolic drug delivery would be particularly beneficial for transcutaneous administration of vaccines because of the efficient antigen uptake by Langheran dendritic cells.¹⁰ Therefore, we set out to synthesize smaller core-shell nanoparticles to see if we could increase their ability to permeate into the skin. We focused on reducing the diameter of the PDEAEMA core without the PAEMA shell because the core provides the most significant contribution to the particle diameter. We were able to observe a decrease in particle size when we decreased the synthesis duration and monomer concentration; however, our particles were typically larger than the particles reported by Hu et al. (2007). Thus, we were not able to decrease the particle diameter significantly; the smallest particle diameter we observed was 141.2 ± 0.9 nm for the ~ 3 min synthesis at pH 8.17 whereas the smallest particle diameter reported by Hu et al (2007) was 205 ± 5 nm. The manipulation of the

polymerization kinetics might not be the best approach for obtaining significantly smaller particles because they become colloidally unstable. Because the smaller particles have less of a surface charge, the small particles most likely require another mechanism for particle stabilization rather than just electrostatic repulsion. When we created PDEAEMA/PEGMA copolymer nanoparticles, we observed slightly smaller particles. Changing the polymerization kinetics and the relative monomer fraction could allow us to produce smaller particles because the amphiphilic copolymer also provides steric stabilization. Because the drugs are electrostatically adsorbed to the particle surface, the shell composition was believed to be critical in determining type of drugs that can be chaperoned by the core-shell nanoparticles. Therefore, we wanted to observe the flexibility in the shell composition to see whether the nanoparticles could be tailored towards a variety of potential drugs. We synthesized three sets of nanoparticles with different shell compositions: polar PEGMA, negatively charged MAA/PEGMA shell, and a positively charged AEMA/PEGMA shell. Surprisingly, the particles with the different charged shells all exhibited similar zeta potentials, which mostly reflected the surface charge density of the PDEAEMA core. When we synthesized nanoparticles with a smaller PDEAEMA core and a thicker PAEMA shell, we were able to observe a change in the zeta potential that was consistent with the larger positive surface charge density and the higher pK_b of the PAEMA shell. This suggests that the adsorption of positively charged drugs may be difficult because it would require negatively charged shell that is thick enough to counteract the positive PDEAEMA core.

References

1. Jain, S.; Yap, W. T.; Irvine, D. J. *Biomacromolecules*, **2005**, 6, 2590 -2600
2. Tcherniuk, S. O.; Chroboczek, J.; Balakirev, M. Y. *Molecular Therapy*. **2005**, 11, 196–204
3. Medina-Kauwe L. K.; Xie J.; Hamm-Alvarez S. *Gene Therapy*. **2005**, 12, 1734-151.
4. Tagami, T.; Barichello, J. M.; Kikuchi, H.; Ishida, T.; Kiwada, H. *Int. J. Pharm.* **2007**, 333, 62-69.
5. Raychaudhuri, S., and Rock, K. *J. Immunol.* **1998**, 16, 1025-1031.
6. Zarei, S. J. *InVest. Dermatol.* **2003**, 121, 745-750.
7. Uhrich, K. E.; Cannizzaro, S. M.; Langer, R. S.; Shakesheff, K. M. *Chem. ReV.* **1999**, 99, 3181-3198.
8. Hu, Y et al. *Nano Letters*. **2007**, 7, 3056-3064.
9. Sonawane, N. D; Szoka, F. C.; Verkman, A. S. *J. of Biol. Chem.* **2003**, 278, pp. 44826–44831
10. Vicari, A. et al. *Cancer and Inflammation*. **2004**, 241-258
11. Gu, H and Roy, K. *J. of Drug Delivery Sci. and Tech.* **2004**, 14, 265-273.
12. Immanuel, C. D. et al. *Comp. and Chem. Eng.* **2002**, 26, 1133–1152
13. Goodall, A. R.; Wilkinson, M. C.; Hearnm J. *J. of Pol. Sci. Poly Chem. Ed.* **1977**,15, 2193-2218
14. Karlsson, O. J.; Schade, B. E. H. Particle Analysis: Particle Size, Particle Shape and Structure and Surface Characterization. In: van Herk, A. M., eds. *Chemistry and Technology of Emulsion Polymerization*. Ames, Iowa: Blackwell; **2005**, 189-190.
15. Vincent, B. Colloidal Aspects of Emulsion Polymerization. In: van Herk, A. M., eds. *Chemistry and Technology of Emulsion Polymerization*. Ames, Iowa: Blackwell; **2005**: 144-148.
16. Fitch, R. M. Polymer Colloids. American Press; **1997**, 6-28.
17. Xu, X.-J; Chen, F. *Langmuir*. **2004**, 20, 528-531.
18. van Herk, A. M.; Gilbert, B. Emulsion Polymerization. In: van Herk, A. M., eds. *Chemistry and Technology of Emulsion Polymerization*. Ames, Iowa: Blackwell; **2005**: 46-78.
19. Wutzel, H.; Samhaber, W. M. *Monatshefte fu" r Chemie*. **2007**. 138, 357–361.
20. Ceska, G. W. *J. of App. Poly. Sci.* **1974**, 18, 427-437.
21. Van den Hull, H. J.; Vanderhoff, J. W. *Brit. Polym. J.* **1970**, 2,121.